

---

---

# Analysis of Extrastriatal $^{123}\text{I}$ -FP-CIT Binding Contributes to the Differential Diagnosis of Parkinsonian Diseases

Merijn Joling<sup>1-4</sup>, Chris Vriend<sup>1,3-5</sup>, Odile A. van den Heuvel<sup>3-5</sup>, Pieter G.H.M. Raijmakers<sup>6</sup>, Paul A. Jones<sup>7</sup>, Henk W. Berendse<sup>1,3</sup>, and Jan Booij<sup>2,3</sup>

<sup>1</sup>Department of Neurology, VU University Medical Center, Amsterdam, The Netherlands; <sup>2</sup>Department of Nuclear Medicine, Academic Medical Center, Amsterdam, The Netherlands; <sup>3</sup>Amsterdam Neuroscience, Amsterdam, The Netherlands; <sup>4</sup>Department of Anatomy and Neurosciences, VU University Medical Center, Amsterdam, The Netherlands; <sup>5</sup>Department of Psychiatry, VU University Medical Center, Amsterdam, The Netherlands; <sup>6</sup>Department of Radiology and Nuclear Medicine, VU University Medical Center, Amsterdam, The Netherlands; and <sup>7</sup>GE Healthcare, The Grove Centre, Amersham, United Kingdom

$^{123}\text{I}$ -*N*- $\omega$ -fluoropropyl-2 $\beta$ -carbomethoxy-3 $\beta$ -(4-iodophenyl)nortropane ( $^{123}\text{I}$ -FP-CIT) SPECT can visualize and quantify striatal dopamine transporter (DAT) binding in vivo. In addition,  $^{123}\text{I}$ -FP-CIT has modest affinity for the serotonin transporter (SERT), predominantly represented in extrastriatal binding. On the basis of previous imaging studies that have suggested more pronounced degeneration of other monoaminergic systems in multiple-system atrophy (MSA) and progressive supranuclear palsy (PSP) than in Parkinson disease (PD), we hypothesized that, in addition to striatal DAT binding, there would be differences in extrastriatal  $^{123}\text{I}$ -FP-CIT SPECT binding to SERT between MSA, PSP, and PD. **Methods:** We included patients with parkinsonian type MSA (multiple-system atrophy with predominantly parkinsonism [MSA-P],  $n = 9$ ), cerebellar type MSA (MSA-C,  $n = 7$ ), PSP ( $n = 13$ ), and PD ( $n = 30$ ).  $^{123}\text{I}$ -FP-CIT binding was analyzed using region-of-interest (ROI) as well as voxel-based methods in both the DAT-rich striatum (caudate nucleus and putamen) and the SERT-rich extrastriatal brain regions (thalamus, hypothalamus, and pons). For SERT analysis, patients on selective serotonin reuptake inhibitor were excluded ( $n = 48$  remained). **Results:** In the ROI analyses, extrastriatal  $^{123}\text{I}$ -FP-CIT binding ratios in the hypothalamus were significantly lower in PSP than in MSA-C patients, and we observed significantly lower striatal  $^{123}\text{I}$ -FP-CIT binding ratios in the caudate nucleus of PSP patients than in that of both PD and MSA-C patients. In the posterior putamen, binding ratios were significantly lower in MSA-P, PSP, and PD than MSA-C patients. Striatal ROI outcomes were confirmed by the voxel-based analyses that additionally showed a significantly lower hypothalamic binding in PSP and MSA-P than PD. **Conclusion:** Striatal  $^{123}\text{I}$ -FP-CIT binding to DAT and hypothalamic  $^{123}\text{I}$ -FP-CIT binding to SERT are significantly lower in MSA-P and PSP than in PD and MSA-C patients and might therefore be of interest for differential diagnosis.

**Key Words:** Parkinson's disease; multiple system atrophy; progressive supranuclear palsy;  $^{123}\text{I}$ -FP-CIT SPECT; DAT; SERT

**J Nucl Med 2017; 58:1117–1123**

DOI: 10.2967/jnumed.116.182139

**P**arkinson disease (PD) is a common degenerative brain disease that affects approximately 1% of people older than 60 y (1). Loss of dopaminergic neurons in the substantia nigra plays a major role in the etiology of the motor symptoms that characterize PD—that is, bradykinesia, rigidity, postural instability, and resting tremor (2). These motor symptoms are also associated with other degenerative brain diseases in which dopaminergic neurons are affected: progressive supranuclear palsy (PSP; estimated prevalence 6.4/100,000 (3)) and multiple-system atrophy (MSA; estimated prevalence 5.4/100,000 (3)). Clinically and neuropathologically, MSA can be divided into MSA with predominantly parkinsonian features (MSA-P) or with cerebellar features (MSA-C), occurring in an estimated ratio of 2:1, respectively (3). Although MSA-C commonly shows more distinguishable clinical symptoms, the similarity of the motor symptoms in PD, MSA-P, and PSP, especially in the early clinical stages, often makes it difficult to unequivocally establish an accurate clinical diagnosis. Indeed, it is not uncommon that the clinical diagnosis needs to be adjusted during the course of the disease (4), thereby inducing frustrating uncertainty of prognosis and treatment outcomes in patients and health-care professionals.

$^{123}\text{I}$ -*N*- $\omega$ -fluoropropyl-2 $\beta$ -carbomethoxy-3 $\beta$ -(4-iodophenyl)nortropane ( $^{123}\text{I}$ -FP-CIT) is a well-validated SPECT tracer with high affinity for the dopamine transporter (DAT). Studies have shown that  $^{123}\text{I}$ -FP-CIT SPECT scans can visualize loss of nigrostriatal dopaminergic neurons (5). Consequently, this molecular imaging technique can help to distinguish PD, MSA-P, or PSP from other movement disorders not characterized by dopaminergic degeneration (e.g., essential tremor) (6). However, to differentiate between PD, MSA-P, and PSP using DAT imaging by  $^{123}\text{I}$ -FP-CIT SPECT remains a challenge. Although some studies have demonstrated lower striatal DAT binding in MSA-P and PSP patients than in PD patients, findings have so far been inconsistent (4,6–14). Moreover, at the individual level there is a clear overlap in binding ratios between MSA-P, PSP, and PD patients, which precludes a role for striatal DAT imaging with  $^{123}\text{I}$ -FP-CIT SPECT to differentiate between degenerative parkinsonian diseases in daily clinical practice.

In addition to its affinity for DAT,  $^{123}\text{I}$ -FP-CIT also has a modest affinity for the serotonin transporter (SERT) (15), which is located on the presynaptic membrane of serotonergic neurons (16).  $^{123}\text{I}$ -FP-CIT binding to SERT is predominantly visible in extrastriatal regions: the diencephalon (hypothalamus and thalamus), the midbrain, and the pons (17–19). Lower midbrain SERT binding has been reported

---

Received Aug. 3, 2016; revision accepted Nov. 7, 2016.  
For correspondence or reprints contact: Merijn Joling, VU University Medical Center, Department of Neurology, P.O. Box 7057, 1007 MB Amsterdam, The Netherlands.  
E-mail: me.joling@vumc.nl  
Published online Nov. 17, 2016.  
COPYRIGHT © 2017 by the Society of Nuclear Medicine and Molecular Imaging.

for PSP (20) and MSA-P (10) in comparison to PD, using  $^{123}\text{I}$ -FP-CIT and  $^{123}\text{I}$ - $\beta$ -CIT, respectively, a radiotracer chemically similar to  $^{123}\text{I}$ -FP-CIT. In this cross-sectional study, we therefore analyzed both striatal and extrastriatal  $^{123}\text{I}$ -FP-CIT binding in patients with PD, PSP, MSA-P, and MSA-C. We hypothesized that both striatal and extrastriatal  $^{123}\text{I}$ -FP-CIT binding would be lower in PSP and MSA-P than in PD and MSA-C.

## MATERIALS AND METHODS

### Participants

We performed a cross-sectional study on consecutive cases presented between May 2008 and December 2015 to the outpatient clinic for movement disorders of the VU University Medical Center (VUmc) in Amsterdam, The Netherlands. Clinical data—and for some patients,  $^{123}\text{I}$ -FP-CIT SPECT scans—were acquired, and a consensus diagnosis was established by a multidisciplinary team including movement disorders specialists. A clinical diagnosis of PD was based on the U.K. PD Society Brain Bank criteria (2,21). For MSA-P and MSA-C, revised American Autonomic Society/American Academy of Neurology criteria (22) were used; a diagnosis of PSP was established using the National Institute of Neurologic Disorders and Stroke and Society for Progressive Supranuclear Palsy criteria (23). After patients provided informed consent, all data were registered in a pseudonymized database for research purposes. This procedure was approved by the local Medical Ethics Committee of VUmc.

We made a selection from this database of parkinsonian patients for whom an  $^{123}\text{I}$ -FP-CIT SPECT scan was available. The initial clinical diagnosis was confirmed with their medical records. Patients no longer returning to VUmc for clinical follow-up were approached by letter, and their current clinical diagnosis was retrieved from their neurologist. This procedure was approved by the local Medical Ethics Committee of VUmc. Of all patients meeting selection criteria, 16 had a clinical diagnosis of MSA (9 MSA-P and 7 MSA-C) and 13 of PSP. MSA and PSP patients were age- and sex-matched with 30 PD patients, selected from the research database, masked for  $^{123}\text{I}$ -FP-CIT SPECT scan outcome.

### Clinical Characteristics

We assessed severity of motor symptoms using the Unified Parkinson's Disease Rating Scale, motor evaluation (24). The Scale for Outcomes of Parkinson's Disease—Autonomic Symptoms subscale was used to assess autonomic symptoms (25). Hoehn and Yahr (26) disease stages were determined for PD patients only, because this scale was specifically designed for PD. Disease duration was defined as the time between the onset of motor symptoms, as subjectively reported by the patients, and the day of  $^{123}\text{I}$ -FP-CIT imaging.

### $^{123}\text{I}$ -FP-CIT SPECT Image Acquisition and Preprocessing

$^{123}\text{I}$ -FP-CIT scans were acquired and preprocessed as described earlier by Vriend et al. (27). In short, 3–4 h before images were acquired,  $^{123}\text{I}$ -FP-CIT was intravenously administered in a dose of approximately 185 MBq (specific activity > 185 MBq/nmol; radiochemical purity > 99%; produced as DaTSCAN according to good-manufacturing-practices criteria at GE Healthcare, Eindhoven, The Netherlands). Static images were obtained for 30 min using a dual-head  $\gamma$ -camera (E.Cam; Siemens) with a fanbeam collimator. Reconstructed images were subsequently reoriented and normalized to Montreal Neurological Institute space using Statistical Parametric Mapping 8 software (Wellcome Trust Centre for Neuroimaging) with a standardized in-house  $^{123}\text{I}$ -FP-CIT SPECT template as described by Vriend et al. (28).

### $^{123}\text{I}$ -FP-CIT SPECT Image Analysis

*Region-of-Interest (ROI) Analyses.* We defined ROIs for the DAT-rich caudate nucleus and the SERT-rich thalamus from the automated

anatomical labeling atlas; the DAT-rich posterior putamen was based on the putamen in this atlas as described elsewhere (27). We based the SERT-rich pons ROI on the Talairach Daemon (TD) Lobes atlas; and the SERT-rich hypothalamus was based on the TD Brodmann area + atlas, and because of its small size, this region was 2 times dilated. All ROIs were implemented in the WFU Pickatlas (version 3.0.5; Wake Forest University) (Supplemental Fig. 1; supplemental materials are available at <http://jnm.snmjournals.org>). We used nonspecific  $^{123}\text{I}$ -FP-CIT binding in the cerebellum as a reference (REF; WFU Pickatlas, automated anatomical labeling atlas; bilateral Crus 2). The ratios of specific to nonspecific binding (binding ratios) were calculated using Statistical Parametric Mapping 8 software by [(ROI – REF)/REF] and used as outcome measures.

*Analysis with DaTQUANT.* In routine clinical practice, software is commonly used to automatically analyze striatal DAT binding, which offers the practical advantage that time-consuming preprocessing steps are not needed. Therefore, we also used the DaTQUANT image quantification software, developed by GE Healthcare, to analyze the striatal DAT binding. This software package is written with the posterior putamen and caudate nucleus as standard ROIs and binding activity in the occipital lobe as a reference. Specific-to-nonspecific binding ratios in the striatum were calculated as described by Siepel et al., using [(mean counts ROI – mean counts reference)/(mean counts occipital lobe)] (29).

*Voxel-Based Analyses.* In addition to the ROI analyses, we performed voxel-based analyses on the ROIs that showed significant between-group differences using the ROI approach. All voxels in the  $^{123}\text{I}$ -FP-CIT SPECT scan were adjusted by the mean binding in the cerebellar reference region according to [(voxel – REF)/REF]. Voxel-based between-group analyses were performed using Statistical Parametric Mapping 8 software and explicitly masked for the relevant ROI. The statistical threshold was set to a *P* value of less than 0.05, family wise error-corrected for multiple comparisons. Age was included as a nuisance covariate in all analyses.

### Statistics

Because selective serotonin reuptake inhibitors (SSRIs) can influence striatal and extrastriatal  $^{123}\text{I}$ -FP-CIT SERT binding (17), we performed the extrastriatal group analyses after the patients using SSRIs were excluded ( $n = 48$ : without SSRIs). Striatal analyses were performed with and without patients using SSRIs to assert its influence. For the ROI and DaTQUANT analyses, normality of data was assessed by plotting histograms, examining Q-Q plots, and using the Kolmogorov–Smirnov test for normality. We used 1-way ANOVA tests where appropriate. We used Hochberg GT2 correction for the post hoc tests and set the  $\alpha$ -level to  $P < 0.05$ . Although all groups were matched for age, we performed additional analysis of covariance to test for the influence of interindividual age differences on  $^{123}\text{I}$ -FP-CIT binding. Assumptions for analysis of covariance were met; including homogeneity of the variances and regression slopes. We analyzed data that did not approximate a normal distribution by the nonparametric Kruskal–Wallis tests. We performed  $\chi^2$  tests to test for equal distribution of sex among the groups. For ROI analyses and patient characteristics, we used SPSS 22 (IBM Corp.).

## RESULTS

### Group Characteristics

Group characteristics are summarized in Table 1. There were no significant group differences in sex ( $\chi^2_3 = 2.986$ ,  $P = 0.394$ ) and disease duration (Kruskal–Wallis test = 4.98,  $P = 0.173$ ). There was a slight difference in age ( $F_{3,55} = 2.322$ ,  $P = 0.085$ ), where the MSA-P group was younger. PD patients had a median Hoehn and Yahr score of 2.5 (interquartile range, 1.5). SSRIs—comprising

**TABLE 1**  
Clinical Characteristics

Characteristic	PD	MSA-P	MSA-C	PSP	Test statistic/df/P
No. of patients	30	9	7	13	
Sex					$\chi^2 = 2.986/3/0.394$
Female	14	7	4	6	
Male	16	2	3	7	
Age at DAT SPECT	66.39 ± 7.55	61.37 ± 9.61	67.72 ± 10.63	70.46 ± 6.29	F = 2.322/3,55/0.085
Disease duration (y)	3.59 ± 2.95	3.15 ± 2.59	3.57 ± 1.43	5.69 ± 4.71	Kruskal–Wallis test = 4.98/3/0.173
UPDRS III	26.8 ± 12.4	41.38 ± 22.83	36.50 ± 7.78	33.17 ± 12.13	Kruskal–Wallis test = 6.58/3/0.087
SCOPA-AUT	35.57 ± 8.45	44.88 ± 12.05	53.00 ± 11.31	36.62 ± 6.62	F = 12.662/2,55/0.001*
SSRI (n)	5 (16.7)	3 (33.3)	0 (0)	3 (23.1)	

\*For this analysis MSA-P and MSA-C were pooled into 1 group.  
df = degree of freedom; UPDRS III = Unified Parkinson's Disease Rating Scale, motor evaluation; SCOPA-AUT = SScale for Outcomes of Parkinson's Disease–AUTonomic Symptoms.  
Values are mean ± SD, unless otherwise specified. Data in parentheses are percentages.

citalopram ( $n = 5$ ), paroxetine ( $n = 2$ ), sertraline ( $n = 2$ ), fluvoxamine ( $n = 1$ ), and fluoxetine ( $n = 1$ )—were used by 5 PD (16.7%), 3 MSA-P (33.3%), and 3 PSP (23.1%) patients on the day of scanning. Excluding SSRI users had an effect on disease duration only, explained by a longer duration in PSP patients than the other parkinsonisms (Kruskal–Wallis test = 8.785,  $P = 0.032$ ).

#### ROI-Based $^{123}\text{I}$ -FP-CIT SPECT Analyses

**Striatal DAT Binding.** We found a significant between-group difference in  $^{123}\text{I}$ -FP-CIT binding ratios for all 4 striatal ROIs, corrected for age (caudate right,  $F_{3,55} = 6.621$ ,  $P = 0.001$ ; caudate left,  $F_{3,55} = 7.619$ ,  $P < 0.001$ ; posterior putamen right,  $F_{3,55} = 6.588$ ,  $P = 0.001$ ; posterior putamen left,  $F_{3,55} = 7.559$ ,  $P < 0.001$ ) (Table 2). Post hoc analyses showed lower  $^{123}\text{I}$ -FP-CIT binding ratios in PSP in the bilateral caudate nuclei ( $P = 0.010$  right,

$P = 0.001$  left) and a trend toward lower binding ratios in the caudate of MSA-P patients ( $P = 0.081$  right,  $P = 0.078$  left) than in PD patients. MSA-C patients showed higher striatal binding ratios than PSP (caudate,  $P = 0.005$  right,  $P = 0.004$  left; and posterior putamen,  $P = 0.003$  right,  $P = 0.001$  left), MSA-P (posterior putamen,  $P = 0.002$  right,  $P = 0.001$  left), and PD (left posterior putamen,  $P = 0.020$ ) patients (Fig. 1). Excluding patients on SSRIs had no effect on these reported results (data not shown).

Consistent with our ROI analysis, the DaTQUANT analysis showed between-group differences in the right posterior putamen, however, not on the left side ( $F_{3,55} = 6.046$ ,  $P = 0.001$  right;  $F_{3,55} = 0.877$ ,  $P = 0.459$  left). There were higher binding ratios in PD than in PSP patients in the bilateral caudate nuclei ( $P = 0.035$  right,  $P = 0.044$  left) and at trend-significant level in the left caudate nucleus ( $P = 0.067$ ) compared with MSA-P patients. Patients with MSA-C

**TABLE 2**  
Between-Group Differences in  $^{123}\text{I}$ -FP-CIT Binding

ROIs	PD	MSA-P	MSA-C	PSP	F/df/P
<b>Striatal</b>					
Caudate left	1.82 ± 0.37	1.39 ± 0.47	1.99 ± 0.54	1.22 ± 0.53	7.619/3,55/<0.001
Caudate right	1.89 ± 0.41	1.43 ± 0.54	2.16 ± 0.55	1.36 ± 0.56	6.621/3,55/0.001
Putamen left	1.57 ± 0.33	1.22 ± 0.51	2.12 ± 0.51	1.28 ± 0.52	7.559/3,55/<0.001
Putamen right	1.49 ± 0.39	1.08 ± 0.50	1.95 ± 0.46	1.18 ± 0.54	6.588/3,55/0.001
<b>Extrastriatal</b>					
Hypothalamus	0.67 ± 0.16	0.45 ± 0.28	0.78 ± 0.30	0.47 ± 0.28	4.307/3,43/0.012
Thalamus left	0.79 ± 0.18	0.58 ± 0.27	0.80 ± 0.29	0.70 ± 0.29	1.576/3,43/0.236
Thalamus right	0.81 ± 0.18	0.68 ± 0.24	0.90 ± 0.20	0.68 ± 0.26	2.332/3,43/0.087
Pons	0.55 ± 0.03	0.41 ± 0.09	0.50 ± 0.05	0.48 ± 0.07	0.803/3,43/0.375

Extrastriatal groups depicted for patients without SSRI; F, df, and P values given are between-group analysis of covariance results, corrected for age.

Values given are mean ± SD, unless otherwise specified.  
df = degrees of freedom.

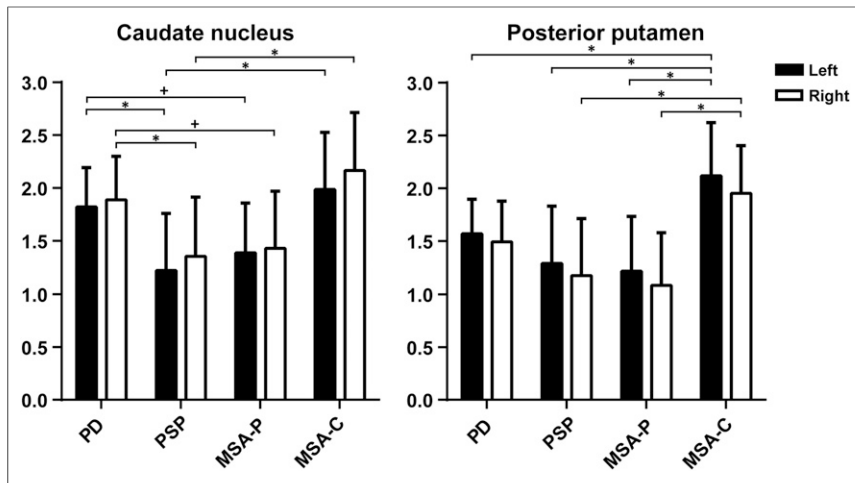


**FIGURE 1.** Binding ratios per ROI. \* = statistically significant difference; + = trend. Striatal regions, including patients using SSRIs.

had higher binding ratios than PSP patients in the bilateral caudate nuclei (MSA-C vs. PSP,  $P = 0.004$  right,  $P = 0.008$  left; MSA-C vs. MSA-P,  $P = 0.022$  right,  $P = 0.011$  left) and the right posterior putamen (MSA-C vs. PSP,  $P = 0.006$ ; MSA-C vs. MSA-P,  $P = 0.001$ ). MSA-C also showed higher binding ratios than PD in the right posterior putamen ( $P = 0.012$ ).

**Extrastriatal SERT Binding.**  $^{123}\text{I}$ -FP-CIT binding differed significantly between diagnostic groups in the hypothalamus ( $F_{3,43} = 4.307$ ,  $P = 0.010$ ) but in none of the other extrastriatal ROIs (Table 2). The group difference in hypothalamic binding was due to higher binding ratios in MSA-C patients than in PSP patients ( $P = 0.044$ ) and MSA-P patients at trend-significant level ( $P = 0.065$ ) (Fig. 2 for hypothalamus; Supplemental Fig. 2 for other regions).

#### Voxelwise $^{123}\text{I}$ -FP-CIT SPECT Imaging Analysis

**Striatal DAT Binding.** We observed significant between-group differences in striatal  $^{123}\text{I}$ -FP-CIT binding ratios. Binding ratios were higher in the caudate nucleus of PD patients than in both caudate nuclei of PSP patients and in the right caudate nucleus of MSA-P patients. MSA-C patients had higher binding ratios than PSP patients (both caudate nuclei) and MSA-P patients (right caudate nucleus). In the posterior putamen, MSA-C patients showed bilaterally higher  $^{123}\text{I}$ -FP-CIT binding ratios than all other groups; PD patients showed higher  $^{123}\text{I}$ -FP-CIT binding ratios than PSP patients in the right posterior putamen (Table 3; Supplemental Figs. 3–6).

**Extrastriatal SERT Binding.** Figure 3 shows the results of the between-group analysis for the hypothalamus. Post hoc tests revealed that PD and MSA-C patients had higher binding ratios than PSP and MSA-P patients (Table 3).

#### MRI Scans

MRI scans of the brain were available for 10 of 13 PSP patients (77%): 6 scans showed mesencephalic atrophy, typical for PSP, and 4 were rated as normal. MRI scans were also available for 6 of the 9 MSA-P patients (67%)—2 scans showed atrophy in the basal ganglia, 1 showed cerebellar atrophy with a hot-cross bun sign, typical for MSA, and 3 showed global cortical atrophy. Brain MR images were available for 5 of the 7 (71%) examined MSA-C patients, which showed atrophy of the cerebellum, except for 1 that showed global cortical atrophy. MRI scans were available in 24 of the 30 examined PD patients (80%): in 18 PD patients, the

MRI scan showed no atrophy, whereas 4 scans showed slight global cortical atrophy and 2 had a more advanced global cortical atrophy.

#### DISCUSSION

The current study explored the use of both striatal and extrastriatal binding ratios derived from a single  $^{123}\text{I}$ -FP-CIT SPECT scan to help distinguish between patients with clinical diagnoses of PD, MSA-P, MSA-C, and PSP.  $^{123}\text{I}$ -FP-CIT binding ratios in the caudate, putamen, and hypothalamus were significantly lower in PSP and MSA-P patients than in PD or MSA-C patients.

In the striatal analysis, we found significantly lower  $^{123}\text{I}$ -FP-CIT binding ratios in the caudate nucleus of PSP patients in comparison to PD patients, and a trend-significant

difference in caudate binding between MSA-P and PD patients. Several previous studies have demonstrated lower overall striatal DAT binding in PSP and MSA-P than PD, with relative sparing of the caudate nucleus in PD (4,8,9,14). Already in early disease stages, patients initially diagnosed with PD that later converted to MSA or PSP have lower DAT binding in the caudate nucleus than patients in whom a diagnosis of PD is maintained (4). In addition, our findings in the posterior putamen in the ROI analysis corroborate the results of earlier studies by Oh and Messa (8,9). The automated DAT binding analyses resulted in comparable data, suggesting this type of approach is useful when assessing striatal binding in routine clinical practice.

In the present study, ROI-based analysis revealed lower extrastriatal  $^{123}\text{I}$ -FP-CIT binding in the hypothalamus in PSP patients and a trend toward lower binding in MSA-P patients, both compared with MSA-C patients. This finding was confirmed by our voxel-based analysis, although this analysis additionally showed lower  $^{123}\text{I}$ -FP-CIT binding in PSP and MSA-P patients than PD patients. This is likely due to the difference in the method of the binding ratio calculation (i.e., mean binding vs. voxelwise). When the results of both analyses were combined, hypothalamic SERT availability appears to be reduced in MSA-P and PSP patients compared with PD and MSA-C patients.

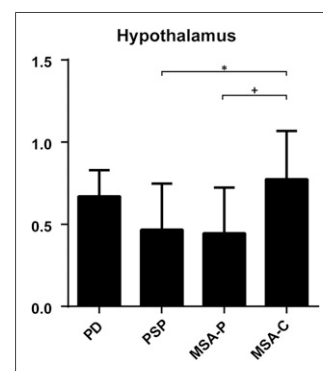


**FIGURE 2.** Binding ratios in hypothalamus, without patients using SSRIs. Data on thalamus and pons are provided in supplemental materials.

Literature on the role of extrastriatal SERT in the differential diagnosis of PD, MSA, and PSP is scarce. Nevertheless, higher SERT binding has been observed in the midbrain and pons of PD patients relative to MSA-P and PSP patients (10,20), and whole brain analysis has been reported to be informative before (14). In the hypothalamus, SERT has been shown to be ubiquitously present in controls in a post-mortem human brain study (30). In line with this, PET studies using selective SERT

**TABLE 3**  
Voxel-by-Voxel Analyses

Region	Group 1 > group 2		$K_e$	$P_{FWE}$ peak-voxel	$T$	x/y/z (mm)
Caudate nucleus left (df, 1,54)	PD	PSP	13	0.005	4.80	-14/4/20
	MSA-C	PSP	4	0.008	4.67	-12/18/12
Caudate nucleus right (df, 1,54)	PD	PSP	22	0.005	4.85	12/4/20
		MSA-P	2	0.024	4.30	16/0/24
Posterior putamen left (df, 1,54)	MSA-C	PSP	2	0.018	4.41	18/0/18
	MSA-C	PSP	41	0.004	4.69	-26/-2/4
Posterior putamen left (df, 1,54)		MSA-P	16	0.007	4.51	-26/-2/4
		PD	33	0.003	4.83	-26/-14/6
Posterior putamen right (df, 1,54)	PD	PSP	2	0.018	4.17	36/-16/-8
	MSA-C	PSP	30	0.004	4.73	28/-10/2
Posterior putamen right (df, 1,54)		MSA-P	28	0.001	5.22	28/-10/2
			13	0.002	4.88	32/-12/8
Hypothalamus* (df, 1,43)		PD	20	<0.001	5.73	28/-10/2
	PD	PSP	17	<0.001	5.93	-4/0/-10
Hypothalamus* (df, 1,43)		MSA-P	6	0.002	4.79	-6/0/-10
	MSA-C	PSP	8	<0.001	5.47	-2/0/-8
Hypothalamus* (df, 1,43)		MSA-P	4	0.002	4.79	-6/0/-10

\*For this analysis, patients not on SSRIs were included.

Difference between 2 diagnoses for specific cluster.

df =degrees of freedom;  $K_e$  = cluster extent in no. of voxels;  $P_{FWE}$  = familywise error-corrected  $P$  values;  $T$  =  $T$  statistic; x/y/z = location of significantly most different between-groups cluster from midpoint in millimeter.

tracers as well as an  $^{123}\text{I}$ -FP-CIT SPECT study have shown specific hypothalamic binding in healthy controls (31,32). Moreover,  $^{123}\text{I}$ -FP-CIT binding in the hypothalamus of rats could be blocked with an SSRI, but not with a DAT blocker (5). Therefore, it is likely that  $^{123}\text{I}$ -FP-CIT binding in the hypothalamus represents predominantly binding to the SERT.

Regarding observations on the role of serotonin in the hypothalamus in MSA or PSP patients, loss of serotonergic neurons in the hypothalamus has been shown in an autopsy study in MSA (33). Chinaglia et al. (34) found a decrease of SERT binding in the cortex and caudate nucleus in PSP, although findings were not consistent (35). Nevertheless, although no autopsy study looked specifically into SERT expression in the hypothalamus in MSA or PSP, our present data may motivate examination of SERT in the hypothalamus in future autopsy studies.

Data on hypothalamic tracer binding in the differential diagnosis is also not abundant, yet lower in vivo SERT availability in the hypothalamus of MSA patients than healthy controls, lower hypothalamic  $^{18}\text{F}$ -FP-CIT binding (reflecting predominantly SERT binding) in PSP than in PD patients, and lower SERT-specific  $^{11}\text{C}$ -DASB binding (which reflects SERT binding, because  $^{11}\text{C}$ -DASB is a selective SERT tracer) in PD patients than healthy controls have been reported previously (36–38). To our knowledge, a  $^{11}\text{C}$ -DASB PET study that examined the availability of SERT in the hypothalamus in MSA or PSP as compared with PD has not been performed before.

The hypothalamus is an important brain area for autonomic functions, such as the stress responses: these functions are partly regulated by serotonin (39). Because patients with MSA-P have

prominent autonomic symptoms and neuronal inclusion bodies have been demonstrated in the hypothalamus in both MSA-P and MSA-C (40), a logical assumption would be that loss of SERT-expressing neurons, represented by lower  $^{123}\text{I}$ -FP-CIT binding, accounts for dysregulation of these autonomic functions in MSA-P. Although some studies looked into the relationship between loss of serotonin and autonomic symptoms in MSA, to our

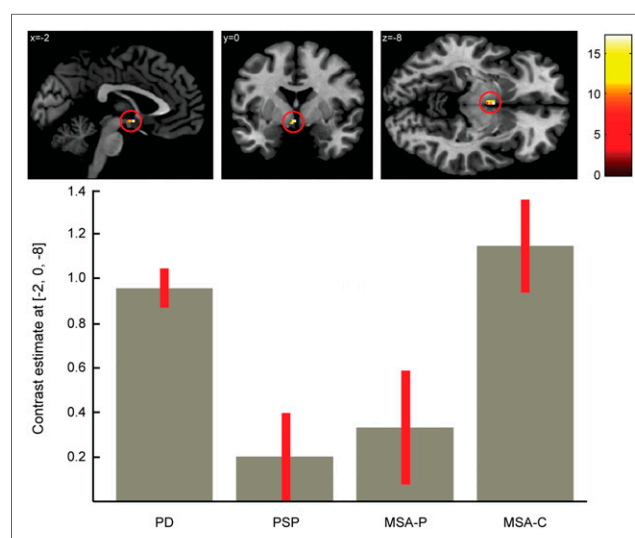


**FIGURE 3.** Voxel-by-voxel analysis of hypothalamus at (x,y,z), -2,0,-8. (Lower) Quantification per diagnosis.

knowledge, no studies examined the role of serotonin in the hypothalamus in PSP. However, our present data may underscore the need to look into this in future studies.

We observed marked differences in both striatal DAT and extrastriatal SERT binding ratios when comparing MSA-P with MSA-C patients, with overall higher binding ratios in MSA-C patients. In fact, 2 MSA-C patients had scan results that in the clinic were diagnostically rated as normal, something that has also been observed previously (Supplemental Fig. 7) (41,42). Our results are consistent with another study that observed less severe loss of DAT binding in striatal regions in MSA-C compared with MSA-P patients, as measured by  $^{18}\text{F}$ -FP-CIT PET (43). Jakobson Mo et al. found lower striatal  $^{123}\text{I}$ -FP-CIT binding ratios in PD and PSP than in MSA patients; however, they made no distinction between MSA-P and MSA-C, which possibly explains why they found lower binding in PD than in MSA in contrast to our results (6).

Some patients in this study were using SSRIs, which may interfere with striatal  $^{123}\text{I}$ -FP-CIT binding in healthy subjects (17). However, we did not find binding differences when we compared patients using SSRIs with those who did not use SSRIs (data not shown). This has previously been described for PD patients chronically using SSRIs in a comparison with patients not using SSRIs, when corrected for disease duration (44). Apparently, the striatal effects of SSRI use on striatal  $^{123}\text{I}$ -FP-CIT binding are small in chronically treated parkinsonian patients. Considering that the use of SSRIs is a reality in daily clinical practice, in our sample 18.6% of patients were using an SSRI on the day they were scanned. It is important to know that SSRI use in parkinsonian patients is not a confounder in analysis of striatal  $^{123}\text{I}$ -FP-CIT binding ratios. Noticeably, use of an SSRI probably does confound the analysis of extrastriatal binding; therefore, we excluded SSRI users from our extrastriatal analysis.

A limitation of this study is the fact that the limited resolution of SPECT cameras might impede an accurate measurement of small areas such as the hypothalamus. To cope with this, we dilated the mask of the hypothalamus. Nevertheless, these results are in need of replication, for example, with the SERT-selective PET tracer  $^{11}\text{C}$ -DASB. Furthermore, we had a small sample size for patients with MSA and PSP, a consequence of the low incidence of MSA and PSP in the population (3). The sample was, however, well documented and most of the patients had a substantial follow-up, which is imperative to deal with the problem of clinical diagnostics for which decision-adjusting symptoms might arise during the course of the disease. Although our study had a retrospective design, which in itself also harbors some limitations, we were able to achieve a relatively high degree of diagnostic certainty. Particularly in the MSA-P patients, the MRI scans showed signs of atrophy in the basal ganglia, which supported the clinical diagnosis. We did not correct for atrophy in this study, because MRI scans were not available for each subject. Consequently, we cannot exclude that part of the loss of DAT binding in the putamen, particularly in the MSA-P patients, is caused by local atrophy

## CONCLUSION

This hypothesis-generating study suggests the presence of information relevant for the difference in pathophysiology, and possibly in the differential diagnosis of PD, PSP, MSA-P, and MSA-C, by examining  $^{123}\text{I}$ -FP-CIT binding in extrastriatal brain areas.

## DISCLOSURE

This study was supported by a research grant from GE Healthcare. Jan Booij is a consultant at GE Healthcare and received research grants from GE Healthcare (paid to the institution). Paul A. Jones is an employee of GE Healthcare. Odile A. van den Heuvel received a speaking fee for a Lilly course. Henk W. Berendse received grant support from Roche. Merijn Joling and Chris Vriend declare no conflict of interest and are in control of the data for this study. No other potential conflict of interest relevant to this article was reported.

## REFERENCES

1. de Lau LM, Breteler MM. Epidemiology of Parkinson's disease. *Lancet Neurol*. 2006;5:525–535.
2. Gibb WR, Lees AJ. The relevance of the Lewy body to the pathogenesis of idiopathic Parkinson's disease. *J Neurol Neurosurg Psychiatry*. 1988;51:745–752.
3. Schrag A, Ben-Shlomo Y, Quinn NP. Prevalence of progressive supranuclear palsy and multiple system atrophy: a cross-sectional study. *Lancet*. 1999;354:1771–1775.
4. Stoffers D, Booij J, Bosscher L, Winogrodzka A, Wolters EC, Berendse HW. Early-stage [ $^{123}\text{I}$ ]beta-CIT SPECT and long-term clinical follow-up in patients with an initial diagnosis of Parkinson's disease. *Eur J Nucl Med Mol Imaging*. 2005;32:689–695.
5. Booij J, Andringa G, Rijks LJ, et al. [ $^{123}\text{I}$ ]FP-CIT binds to the dopamine transporter as assessed by biodistribution studies in rats and SPECT studies in MPTP-lesioned monkeys. *Synapse*. 1997;27:183–190.
6. Jakobson Mo S, Linder J, Forsgren L, Holmberg H, Larsson A, Riklund K. Pre- and postsynaptic dopamine SPECT in idiopathic Parkinsonian diseases: a follow-up study. *Biomed Res Int*. 2013;2013:143532.
7. Kim YJ, Ichise M, Ballinger JR, et al. Combination of dopamine transporter and D2 receptor SPECT in the diagnostic evaluation of PD, MSA, and PSP. *Mov Disord*. 2002;17:303–312.
8. Messa C, Volonte MA, Fazio F, et al. Differential distribution of striatal [ $^{123}\text{I}$ ]beta-CIT in Parkinson's disease and progressive supranuclear palsy, evaluated with single-photon emission tomography. *Eur J Nucl Med*. 1998;25:1270–1276.
9. Oh M, Kim JS, Kim JY, et al. Subregional patterns of preferential striatal dopamine transporter loss differ in Parkinson disease, progressive supranuclear palsy, and multiple-system atrophy. *J Nucl Med*. 2012;53:399–406.
10. Scherfler C, Seppi K, Donnemiller E, et al. Voxel-wise analysis of [ $^{123}\text{I}$ ]beta-CIT SPECT differentiates the Parkinson variant of multiple system atrophy from idiopathic Parkinson's disease. *Brain*. 2005;128:1605–1612.
11. Van Laere K, Casteels C, De Ceuninck L, et al. Dual-tracer dopamine transporter and perfusion SPECT in differential diagnosis of parkinsonism using template-based discriminant analysis. *J Nucl Med*. 2006;47:384–392.
12. Varrone A, Marek KL, Jennings D, Innis RB, Seibyl JP. [ $^{123}\text{I}$ ]beta-CIT SPECT imaging demonstrates reduced density of striatal dopamine transporters in Parkinson's disease and multiple system atrophy. *Mov Disord*. 2001;16:1023–1032.
13. Brücke T, Asenbaum S, Pirker W, et al. Measurement of the dopaminergic degeneration in Parkinson's disease with [ $^{123}\text{I}$ ]beta-CIT and SPECT: correlation with clinical findings and comparison with multiple system atrophy and progressive supranuclear palsy. *J Neural Transm Suppl*. 1997;50:9–24.
14. Badoud S, Van De Ville D, Nicastro N, Garibotto V, Burkhard PR, Haller S. Discriminating among degenerative parkinsonisms using advanced  $^{123}\text{I}$ -ioflupane SPECT analyses. *Neuroimage Clin*. 2016;12:234–240.
15. Abi-Dargham A, Gandelman MS, DeErausquin GA, et al. SPECT imaging of dopamine transporters in human brain with iodine-123-fluoroalkyl analogs of beta-CIT. *J Nucl Med*. 1996;37:1129–1133.
16. Torres GE, Gainetdinov RR, Caron MG. Plasma membrane monoamine transporters: structure, regulation and function. *Nat Rev Neurosci*. 2003;4:13–25.
17. Booij J, de Jong J, de Bruin K, Knol R, de Win MM, van Eck-Smit BL. Quantification of striatal dopamine transporters with  $^{123}\text{I}$ -FP-CIT SPECT is influenced by the selective serotonin reuptake inhibitor paroxetine: a double-blind, placebo-controlled, crossover study in healthy control subjects. *J Nucl Med*. 2007;48:359–366.
18. Ziebell M, Holm-Hansen S, Thomsen G, et al. Serotonin transporters in dopamine transporter imaging: a head-to-head comparison of dopamine transporter SPECT radioligands  $^{123}\text{I}$ -FP-CIT and  $^{123}\text{I}$ -PE2I. *J Nucl Med*. 2010;51:1885–1891.
19. Koopman KE, la Fleur SE, Fliers E, Serlie MJ, Booij J. Assessing the optimal time point for the measurement of extrastriatal serotonin transporter binding with  $^{123}\text{I}$ -FP-CIT SPECT in healthy, male subjects. *J Nucl Med*. 2012;53:1087–1090.

20. Roselli F, Pisciotto NM, Pennelli M, et al. Midbrain SERT in degenerative parkinsonisms: a  $^{123}\text{I}$ -FP-CIT SPECT study. *Mov Disord.* 2010;25:1853–1859.
21. Hughes AJ, Daniel SE, Kilford L, Lees AJ. Accuracy of clinical diagnosis of idiopathic Parkinson's disease: a clinico-pathological study of 100 cases. *J Neurol Neurosurg Psychiatry.* 1992;55:181–184.
22. Gilman S, Wenning GK, Low PA, et al. Second consensus statement on the diagnosis of multiple system atrophy. *Neurology.* 2008;71:670–676.
23. Litvan I, Agid Y, Calne D, et al. Clinical research criteria for the diagnosis of progressive supranuclear palsy (Steele-Richardson-Olszewski syndrome): report of the NINDS-SPSP international workshop. *Neurology.* 1996;47:1–9.
24. Fahn S, Elton R. Unified Parkinson's disease rating scale. In: Fahn S, Marsden CD, Calne DB, Goldstein M, eds. *Recent Developments in Parkinson's Disease.* Vol 2. Florham Park, NJ: Macmillan Healthcare Information; 1987:153–163.
25. Visser M, Marinus J, Stiggelbout AM, Van Hilten JJ. Assessment of autonomic dysfunction in Parkinson's disease: the SCOPA-AUT. *Mov Disord.* 2004;19:1306–1312.
26. Hoehn MM, Yahr MD. Parkinsonism: onset, progression and mortality. *Neurology.* 1967;17:427–442.
27. Vriend C, Nordbeck AH, Booij J, et al. Reduced dopamine transporter binding predates impulse control disorders in Parkinson's disease. *Mov Disord.* 2014;29:904–911.
28. Vriend C, Raijmakers P, Veltman DJ, et al. Depressive symptoms in Parkinson's disease are related to reduced  $^{123}\text{I}$ FP-CIT binding in the caudate nucleus. *J Neurol Neurosurg Psychiatry.* 2014;85:159–164.
29. Siepel FJ, Dalen I, Gruner R, et al. Loss of dopamine transporter binding and clinical symptoms in dementia with Lewy bodies. *Mov Disord.* 2016;31:118–125.
30. Borgers AJ, Koopman KE, Bisschop PH, et al. Decreased serotonin transporter immunoreactivity in the human hypothalamic infundibular nucleus of overweight subjects. *Front Neurosci.* 2014;8:106.
31. Kupers R, Frokjaer VG, Erritzoe D, et al. Serotonin transporter binding in the hypothalamus correlates negatively with tonic heat pain ratings in healthy subjects: A  $^{11}\text{C}$ -DASB PET study. *Neuroimage.* 2011;54:1336–1343.
32. Borgers AJ, Alkemade A, Van de Giessen EM, et al. Imaging of serotonin transporters with  $^{123}\text{I}$ FP-CIT SPECT in the human hypothalamus. *EJNMMI Res.* 2013;3:34.
33. Benarroch EE, Schmeichel AM, Low PA, Parisi JE. Depletion of putative chemosensitive respiratory neurons in the ventral medullary surface in multiple system atrophy. *Brain.* 2007;130:469–475.
34. Chinaglia G, Landwehrmeyer B, Probst A, Palacios JM. Serotonergic terminal transporters are differentially affected in Parkinson's disease and progressive supranuclear palsy: an autoradiographic study with  $^3\text{H}$ citalopram. *Neuroscience.* 1993;54:691–699.
35. Landwehrmeyer B, Palacios JM. Alterations of neurotransmitter receptors and neurotransmitter transporters in progressive supranuclear palsy. *J Neural Transm Suppl.* 1994;42:229–246.
36. Berding G, Brucke T, Odin P, et al.  $^{123}\text{I}$ beta-CIT SPECT imaging of dopamine and serotonin transporters in Parkinson's disease and multiple system atrophy. *Nuklearmedizin.* 2003;42:31–38.
37. Jin S, Oh M, Oh SJ, et al. Differential diagnosis of parkinsonism using dual-phase F-18 FP-CIT PET imaging. *Nucl Med Mol Imaging.* 2013;47:44–51.
38. Pavese N, Simpson BS, Metta V, Ramlackhansingh A, Chaudhuri KR, Brooks DJ.  $^{18}\text{F}$ FDOPA uptake in the raphe nuclei complex reflects serotonin transporter availability: a combined  $^{18}\text{F}$ FDOPA and  $^{11}\text{C}$ DASB PET study in Parkinson's disease. *Neuroimage.* 2012;59:1080–1084.
39. Jørgensen HS. Studies on the neuroendocrine role of serotonin. *Dan Med Bull.* 2007;54:266–288.
40. Cykowski MD, Coon EA, Powell SZ, et al. Expanding the spectrum of neuronal pathology in multiple system atrophy. *Brain.* 2015;138:2293–2309.
41. Muñoz E, Iranzo A, Rauek S, et al. Subclinical nigrostriatal dopaminergic denervation in the cerebellar subtype of multiple system atrophy (MSA-C). *J Neurol.* 2011;258:2248–2253.
42. McKinley J, O'Connell M, Farrell M, Lynch T. Normal dopamine transporter imaging does not exclude multiple system atrophy. *Parkinsonism Relat Disord.* 2014;20:933–934.
43. Kim HW, Kim JS, Oh M, et al. Different loss of dopamine transporter according to subtype of multiple system atrophy. *Eur J Nucl Med Mol Imaging.* 2016;43:517–525.
44. Seo M, Oh M, Cho M, Chung SJ, Lee CS, Kim JS. The effect of SSRIs on the binding of  $^{18}\text{F}$ -FP-CIT in Parkinson patients: a retrospective case control study. *Nucl Med Mol Imaging.* 2014;48:287–294.